BULLETIN OF THE POLISH ACADEMY OF SCIENCES
TECHNICAL SCIENCES, Vol. 73(2), 2025, Article number: e153228
DOI: 10.24425/bpasts.2025.153228

Equilibrated residual method for estimation of modelling and approximation errors in complex piezoelectric models

Magdalena ZIELIŃSKA[1]* **and Grzegorz ZBOIŃSKI**[2]

[1] Faculty of Technical Sciences, University of Warmia and Mazury in Olsztyn, Poland
[2] Institute of Fluid-Flow Machinery, Polish Academy of Sciences in Gdańsk, Poland

Abstract. The article presents the equilibrated residual method (ERM) of error estimation in coupled problems in the case of complex piezoelectric models. These models include hierarchical, first-order, and transition models within the mechanical field of displacements, as well as hierarchical models within the electric field of potential. Three (classical, modified and enhanced) transition models are considered. The paper presents a variational formulation of the model problem of general piezoelectricity in the case of complex piezoelectric models and the finite element approximation of this problem. Next, the equilibration residual method for coupled problems of piezoelectricity and complex piezoelectric models is presented. The mechanical, electric and coupled parts of the modelling, approximation and total error estimators, and true errors are given. Effectivity indices (the ratio of estimated error to true error) are used to assess the quality of error estimation in the case of three error parts and three types of error for the complex models of piezoelectric plates. The effectivity results for simple piezoelectric models and uncoupled problems of elasticity and dielectricity are applied as references.

Keywords: piezoelectricity; complex models; finite element method; error estimation; equilibrated residual method.

1. INTRODUCTION

The main objective of the paper is to propose and verify the equilibrated residual method (ERM) of error estimation in the case of piezoelectrics. The ERM estimated error values can be potentially used for the adaptive analysis of simple (one model applied) and complex (multiple models applied) models of piezoelectrics. The simple and complex models are used to model piezoelectric transducers (actuators and sensors). The complex piezoelectric description requires the application of the transition models between the basic (hierarchical and first-order) models. The first (classical) transition model guarantees continuity of displacements on the boundaries between the transition and basic (hierarchical and first-order) models. The second (modified) one allows an additional smooth transition of the stress state between the basic models, while the third (enhanced) one additionally ensures a smooth transition of the strain state between the basic models.

1.1. State of the art

The equilibrated residual method applied to the finite element method (FEM) was developed in [1–3]. Its final version is presented in [4]. The application of ERM to error estimation for elliptic problems was performed in [5] and [6]. Elasticity problems were considered in this context in [7]. ERM error estimation for conventional (mid-surfaces dofs) and 3D-based (through-thickness dofs) models of thin-walled structures were presented in [8] and [9], respectively. Application of the method to 3D-based models of dielectric and piezoelectric structures can be found respectively in [10] and [11].

1.2. Novelty of the paper

Our previous work on the theory and application of the residual equilibrated method considered uncoupled 3D-based problems of elasticity [9] and dielectricity [12, 13]. Next, the method was proposed [13] and applied [10] to coupled 3D-based problems of piezoelectricity. Simple, homogeneous, hierarchical piezoelectric models were used within the latter work. We also suggested the use of ERM for complex piezoelectric models, taking into account the simplest (classical) transition model [14]. Here, we apply the method to the complex piezoelectric models with the use of three different (classical, modified and enhanced) transition models. Also, the homogeneous (basic) piezoelectric model of the first order is applied in the present work.

1.3. The methodology used

The applied ERM error estimation is assigned to the control of model and discretization adaptation within complex 3D-based piezoelectric *hpq*-approximated finite element models. The h, p and q denote element size, and longitudinal and transverse orders of approximation within piezoelectric finite elements. These two orders are defined independently for the mechanical field of displacements and the electric field of potential, while

*e-mail: m.nosarzewska@uwm.edu.pl

Manuscript submitted 2024-10-17, revised 2024-12-06, initially accepted for publication 2024-12-18, published in March 2025.

the size of the element is common for both fields. The applied approach uses hierarchical modelling and hierarchical approximations described in [13]. The starting point for hierarchical modelling and hierarchical approximations was the papers [15] and [16]. Hierarchical models and approximations of piezoelectric basic (hierarchical and first-order) and transition elements were proposed in [10, 13] and [17], respectively. The starting point was the work [18] and [19].

The mentioned hierarchical piezoelectric models are 3D models polynomially constrained through the thickness and applied to thin-walled domains. The order of these polynomial constraints determines the model order. In the case of the first-order model, the hierarchical model must be modified due to the plane-stress assumption and kinematic assumptions within the mechanical field of the piezoelectric.

2. MODEL PROBLEM

2.1. Variational formulation

The variational formulation holds in volume V of the piezoelectric. This volume can be any bounded three-dimensional domain. In this paper, however, we choose the geometry typical for piezoelectric transducers (actuators or sensors), i.e., symmetric-thickness, thin- or thick-walled domains. These domains are defined with the use of the mid-surface and the thickness vector. For such domains elasticities, dielectric constants, anisotropic piezoelectric constants, strains and electric field are defined in two longitudinal and one transverse directions $\alpha,\ \beta,\ \gamma,\ \delta = 1,2,3$, while displacements and forces are defined globally $i,\ j,\ k,\ l = 1,2,3$. In the definition of the piezoelectric constants, the third local direction is the polarization direction. The relation between the global Cartesian and local Cartesian directions reads $x_\alpha = \theta_{\alpha i} x_i$, where $\theta_{\alpha i}$ denotes cosines between the directions of two types. These cosines are consistent with the parametric geometry representation presented in [20] and [21].

The stationarity condition of the electromechanical potential energy functional $\Pi(\boldsymbol{v},\psi)$ reads:

$$\begin{aligned}\Pi(\boldsymbol{v},\psi) = &-B(\boldsymbol{v},\boldsymbol{u}) + C(\boldsymbol{v},\phi) + C(\psi,\boldsymbol{u})\\ &+ b(\psi,\phi) + L(\boldsymbol{v}) - l(\psi) = 0,\end{aligned} \tag{1}$$

where $\boldsymbol{u}$ and ϕ represent solution quantities while $\boldsymbol{v}$ and ψ represent admissible quantities. Above, the first term represents the strain energy, the next two terms denote electro-mechanical coupling energy, the fourth stands for the electric field energy, and the last two terms define the work of external forces and the work of external electric charges. The coupled solution belongs to the following space: $(\boldsymbol{u},\phi) \in U \times \Phi$. The spaces for displacements and electric potential are $U = \left\{\boldsymbol{v} \in \left(H^1(V)\right)^3 : \boldsymbol{v} = \boldsymbol{0} \text{ on } W\right\}$ and $\Phi = \left\{\psi \in H^1(V) : \psi = 0 \text{ on } F\right\}$ with W and F being the supported and grounded parts of the boundary $\partial V \equiv S$ of the volume V.

In the bilinear form:

$$\begin{aligned}B(\boldsymbol{v},\boldsymbol{u}) &= \int_V D^{\alpha\beta\gamma\delta}\varepsilon_{\gamma\delta}(\boldsymbol{u})\varepsilon_{\alpha\beta}(\boldsymbol{v})\,\mathrm{d}V\\ &= \int_V D^{\alpha\beta\gamma\delta}u_{\gamma,\delta}v_{\alpha,\beta}\,\mathrm{d}V.\end{aligned} \tag{2}$$

$D^{\alpha\beta\gamma\delta}$ and $\varepsilon_{\gamma\delta}(\boldsymbol{u})$ $(\alpha,\beta,\gamma,\delta = 1,2,3)$, where $\boldsymbol{u} = \{u_i\}$ and $u_\alpha = \theta_{\alpha i}u_i$ and $u_{\gamma,\delta} = \theta_{\gamma i}u_{i,j}\theta_{j\delta}$, stand for the tensors of elastic constants and local strains, while u_i denotes the global components of the displacement vector $\boldsymbol{u}$. The vector $\boldsymbol{v}$ represents kinematically admissible displacements.

In the mixed forms:

$$\begin{aligned}C(\boldsymbol{v},\phi) &= \int_V C^{\alpha\beta\gamma}E_\gamma(\phi)\varepsilon_{\alpha\beta}(\boldsymbol{v})\,\mathrm{d}V\\ &= \int_V C^{\alpha\beta\gamma}\phi_{,\gamma}v_{\alpha,\beta}\,\mathrm{d}V,\end{aligned} \tag{3}$$

$$\begin{aligned}C(\psi,\boldsymbol{u}) &= \int_V C^{\alpha\gamma\delta}\varepsilon_{\gamma\delta}(\boldsymbol{u})E_\alpha(\psi)\,\mathrm{d}V\\ &= \int_V C^{\alpha\gamma\delta}u_{\gamma,\delta}\psi_{,\alpha}\,\mathrm{d}V,\end{aligned} \tag{4}$$

$C^{\alpha\beta\gamma}$ and $E_\gamma(\phi)$ $(\alpha,\beta,\gamma = 1,2,3)$ stand for the tensor of piezoelectric constants at constant strain [22] and the electric field vector expressed by the potential ϕ. The function ψ represents electrostatically admissible values of this potential.

In the second bilinear form:

$$\begin{aligned}b(\psi,\phi) &= \int_V \gamma^{\alpha\beta}E_\beta(\phi)E_\alpha(\psi)\,\mathrm{d}V\\ &= \int_V \gamma^{\alpha\beta}\phi_{,\beta}\psi_{,\alpha}\,\mathrm{d}V,\end{aligned} \tag{5}$$

$\gamma^{\alpha\beta}$ stands for the tensor of dielectric constants at constant strain [22].

In the linear forms:

$$L(\boldsymbol{v}) = \int_V f^i v_i\,\mathrm{d}V + \int_P p^i v_i\,\mathrm{d}S, \tag{6}$$

$$l(\psi) = \int_Q c\psi\,\mathrm{d}S. \tag{7}$$

f^i and p^i $(i = 1,2,3)$ define external volume and surface forces and c is the external surface electric charge. The symbols P and Q denote the loaded and charged parts of the surface S of the volume V of the piezoelectric, respectively.

2.2. The applied hierarchical, first-order and transition piezoelectric models

In this paper, the complex description of the mechanical field [20] allows for the use of the hierarchical shell model MI, $I \geq 2$, with I standing for the order of the model. Also, the

first-order Reissner-Mindlin (RM) model is applied. Both models are connected by the transition model TR ≡ MI/RM. In the complex description of the electric field [21], the symmetric-thickness hierarchical model EJ, $J \geq 1$ is applied, with J being the order of the model. As a result, the following division $V = V_{\mathrm{M}I,\mathrm{E}J} \cup V_{\mathrm{TR},\mathrm{E}J} \cup V_{\mathrm{RM},\mathrm{E}J}$ holds. In the special case of simple homogeneous models, we will limit ourselves to $V = V_{\mathrm{M}I,\mathrm{E}J}$ or $V = V_{\mathrm{RM},\mathrm{E}J}$.

In all the above-mentioned models, 3D-based approach is applied. This means that the constitutive relations for the hierarchical shell models [20] and hierarchical symmetric-thickness dielectric models [21] are the same as for the 3D elasticity and 3D dielectricity. The displacement and electric potential fields are defined as three-dimensional and are polynomially constrained through the thickness. For the other models, the following modifications presented below must be introduced into hierarchical piezoelectric models.

In the case of the first-order shell model, the following relation of plain stress assumption for the local stress components $\sigma^{\alpha\beta}$, $\alpha,\beta = 1,2,3$ must be introduced into the piezoelectric constitutive relations:

$$\sigma^{33} = D\left[\nu\varepsilon_{11} + \nu\varepsilon_{22} + (1-\nu)\varepsilon_{33}\right] - C_{33}E_3 = 0. \tag{8}$$

Above, $D = E/[(1+\nu)(1-2\nu)]$ with E and ν denoting Young's modulus and Poisson's ratio, C_{33} stands for a non-zero term of the matrix representation of the piezoelectric constants $C^{\alpha\beta\gamma}$, $\alpha,\beta,\gamma = 1,2,3$ under constant strain.

Also, the Reissner-Mindlin kinematic assumption of deformation of the lines normal to the mid-surface and oriented along the third local (transverse) direction x_δ, $\delta = 3$, onto straight lines holds for all three local directions $\alpha = 1,2,3$:

$$u_\alpha = \frac{1}{2}\left(u^b_\alpha + u^t_\alpha\right) + \frac{x_\delta}{t}\left(u^t_\alpha - u^b_\alpha\right). \tag{9}$$

Above, the quantity t in the denominator is the structure thickness. Additionally, the assumption of no elongation of these normal holds:

$$u^t_\delta - u^b_\delta = 0 \tag{10}$$

with $\delta = 3$ denoting the third (transverse) local displacement component. The indices t and b correspond to the top and bottom surfaces of the thin-walled piezoelectric domain.

In the case of the classical transition element, the constitutive relations are three-dimensional and are taken from the hierarchical piezoelectric models.

In the case of the modified and enhanced transition models, the transition from the plane stress to the three-dimensional stress state is assumed for the stress components $\sigma^{\alpha\beta}$ in the local directions $(\alpha,\beta = 1,2,3)$ and described with the relation:

$$\sigma^{33} = -C_{33}E_3 + D\left\{\nu\varepsilon_{11} + \nu\varepsilon_{22} + (1-\nu)\left[\zeta\varepsilon_{33} + (1-\zeta)\left(\frac{-\nu}{1-\nu}(\varepsilon_{11}+\varepsilon_{22}) + \frac{C_{33}}{D(1-\nu)}E_3\right)\right]\right\}, \tag{11}$$

where ζ represents the linear blending function equal to 1 at the boundary with the three-dimensional model and 0 at the boundary with the first-order model.

In the case of the enhanced transition model, the transverse displacement field changes from no elongation of the normals to the mid-surface (at the boundary of the first-order model) to free elongation of these normals (at the boundary with the hierarchical shell model). Now, the function ζ plays the role of a gradually switching function. By this assumption, one can write:

$$u_\alpha = \frac{1}{2}\left(u^0_\alpha + u^I_\alpha\right) + \delta_{\alpha\beta}\frac{x_\delta}{t}\left(u^0_\beta - u^I_\beta\right) + \delta_{\alpha\delta}\zeta\frac{x_\delta}{t}\left(u^0_\delta - u^I_\delta\right) + \zeta\sum_{l=1}^{I-1} f_l(x_\delta)\,u^l_\alpha, \tag{12}$$

where $\alpha = 1,2,3$, $\beta = 1,2$, $\delta = 3$ and $\delta_{\alpha\beta}$, $\delta_{\alpha\delta}$ represent Kronecker deltas, f_l denotes linear ($l = 0$ or $l = I$) or higher-order ($l = 1,2,\ldots,I-1$) polynomials defined in accordance with the displacement field of the hierarchical shell model MI of order I [17].

2.3. Finite element formulation

Equation (1) can be converted into two coupled equations:

$$\begin{cases} B(\boldsymbol{v},\boldsymbol{u}) - C(\boldsymbol{v},\phi) = L(\boldsymbol{v}), \\ -C(\psi,\boldsymbol{u}) - b(\psi,\phi) = -l(\psi). \end{cases} \tag{13}$$

The problem (13), after its finite element approximation, can be described by:

$$\begin{cases} B(\boldsymbol{v}^{hpq},\boldsymbol{u}^{hpq}) - C(\boldsymbol{v}^{hpq},\phi^{h\pi\rho}) = L(\boldsymbol{v}^{hpq}), \\ -C(\psi^{h\pi\rho},\boldsymbol{u}^{hpq}) - b(\psi^{h\pi\rho},\phi^{h\pi\rho}) = -l(\psi^{h\pi\rho}). \end{cases} \tag{14}$$

Above, $(\boldsymbol{u}^{hpq},\phi^{h\pi\rho})$ are the FEM approximation of the solution $(\boldsymbol{u},\phi)$, and $\boldsymbol{v}^{hpq}$ and $\psi^{h\pi\rho}$ stand for the kinematically admissible displacements and the electrostatically admissible potential. The independent longitudinal and transverse orders of approximation of displacements and electric potential are denoted p, q and π, ρ. The error of $(\boldsymbol{u}^{hpq},\phi^{h\pi\rho})$ with respect to $(\boldsymbol{u},\phi)$ is of interest in this work. The numerical solution belongs to the approximated space, i.e., $(\boldsymbol{u}^{hpq},\phi^{h\pi\rho}) \in U^{hpq} \times \Phi^{h\pi\rho}$, where $U^{hpq} = \left\{\boldsymbol{v}^{hpq} \in \left(H^1(V)\right)^3 : \boldsymbol{v}^{hpq} = \boldsymbol{0} \text{ on } W\right\}$ and $\Phi^{h\pi\rho} = \left\{\psi^{h\pi\rho} \in H^1(V) : \psi^{h\pi\rho} = 0 \text{ on } F\right\}$.

The way the assumptions on constitutive relations, displacement field, and electric field are introduced into the finite element formulation of the hierarchical, first-order and three transition elements is presented in [17].

3. ERROR ESTIMATION IN BASIC AND TRANSITION ELEMENTS

In this section, we will apply the equilibrated residual method [4] for error estimation in the basic (hierarchical and first-order) and transition finite elements within complex piezoelectric domains. Following this method, we will investigate the global estimate

and element estimators as well. All estimators will be defined as differences in the potential energies Π corresponding to the ERM estimate $(\hat{u},\hat{\phi})$ of the exact solution $(\boldsymbol{u},\phi)$ and the numerical solution $(\boldsymbol{u}^{hpq},\phi^{h\pi\rho})$.

3.1. Error estimation

The global estimator η is defined as a sum of elemental estimators $\overset{e}{\eta}$ in the following way:

$$\eta = -\Pi\left(\hat{\boldsymbol{u}},\hat{\phi}\right) + \Pi\left(\boldsymbol{u}^{hpq},\phi^{h\pi\rho}\right) = \sum_{e} \overset{e}{\eta}. \tag{15}$$

For any element e, the estimator is equal to

$$\begin{aligned}\overset{e}{\eta} = &-\overset{e}{\Pi}\left(\hat{\boldsymbol{u}},\hat{\phi}\right) - \int\limits_{\overset{e}{S}\setminus S} \hat{\boldsymbol{u}}^T \left\langle \overset{e}{\boldsymbol{r}}(\boldsymbol{u}^{hpq})\right\rangle \mathrm{d}\overset{e}{S} \\ &+ \int\limits_{\overset{e}{S}\setminus S} \hat{\phi}\left\langle \overset{e}{h}(\phi^{h\pi\rho})\right\rangle \mathrm{d}\overset{e}{S} + \overset{e}{\Pi}\left(\boldsymbol{u}^{hpq},\phi^{h\pi\rho}\right),\end{aligned} \tag{16}$$

where the first three terms denote the potential energy of the estimate of the exact solution of the element e. The first term consists of the element energies (strain, electric field and coupling ones) and the work of the external forces and electric charges defined with equations (2)–(7) after the division of the domain V into element subdomains $\overset{e}{V}$, $e = 1,2,\ldots,E$ with E being the total number of elements in the domain. The next two terms represent the work of inter-element reaction stresses $\overset{e}{\boldsymbol{r}}(\boldsymbol{u}^{hpq})$ and equivalent charges $\overset{e}{h}(\phi^{h\pi\rho})$ acting on the internal surfaces $\overset{e}{S}\setminus S$. These stresses and charges are defined in [11] in the way typical for the equilibrated residual method. The fourth term of equation (16) stands for the potential energy of the known numerical solution $(\boldsymbol{u}^{hpq},\phi^{h\pi\rho})$ and it is defined as in [11], i.e.,

$$\begin{aligned}\overset{e}{\Pi}\left(\boldsymbol{u}^{hpq},\phi^{h\pi\rho}\right) = &-\frac{1}{2}\overset{e}{B}\left(\boldsymbol{u}^{hpq},\boldsymbol{u}^{hpq}\right) + \frac{1}{2}\overset{e}{C}\left(\boldsymbol{u}^{hpq},\phi^{h\pi\rho}\right) \\ &+ \frac{1}{2}\overset{e}{C}\left(\phi^{h\pi\rho},\boldsymbol{u}^{hpq}\right) + \frac{1}{2}\overset{e}{b}\left(\phi^{h\pi\rho},\phi^{h\pi\rho}\right).\end{aligned} \tag{17}$$

The above equations (16) and (17) are valid for hierarchical, first-order, and transition piezoelectric elements.

3.2. Local problems of elements

In the case of the total error estimation, the condition of stationarity of the functional from equation (15) (completed with equations (16) and (17)) can be replaced by the element stationarity conditions of the form:

$$\begin{aligned}0 = &-\overset{e}{\Pi}\left(\boldsymbol{v}^{HPQ},\psi^{H\Pi\mathrm{P}}\right) - \int\limits_{\overset{e}{S}\setminus S} \left(\boldsymbol{v}^{HPQ}\right)^T \left\langle \overset{e}{\boldsymbol{r}}(\boldsymbol{u}^{hpq})\right\rangle \mathrm{d}\overset{e}{S} \\ &+ \int\limits_{\overset{e}{S}\setminus S} \psi^{H\Pi\mathrm{P}}\left\langle \overset{e}{h}(\phi^{h\pi\rho})\right\rangle \mathrm{d}\overset{e}{S},\end{aligned} \tag{18}$$

where the global estimate $(\hat{\boldsymbol{u}},\hat{\phi})$ of the exact solution $(\boldsymbol{u},\phi)$ was replaced by a collection of its local finite element approximations $(\boldsymbol{u}^{HPQ},\phi^{H\Pi\mathrm{P}}) \in U^{HPQ}\times\Phi^{H\Pi\mathrm{P}}$. The exact result of the estimation corresponds to $1/H,P,Q \to \infty$ and $1/H,\Pi,\mathrm{P} \to \infty$. In practice, we use lower values, i.e., $H = h$, $P = p+1$, $Q = q+1$ and $\Pi = \pi+1$, $\mathrm{P} = \rho+1$, where h,p,q,π,ρ stand for discretization parameters in the assessed global problem and H,P,Q,Π,P are their counterparts in the local problems.

In turn, in the case of the approximation error ($Q \equiv q$ and $\mathrm{P} \equiv \rho$), the element component of the stationarity condition of the functional from equations (15)–(17) must be defined in the following way:

$$\begin{aligned}0 = &-\overset{e}{\Pi}\left(\boldsymbol{v}^{HPq},\psi^{H\Pi\rho}\right) - \int\limits_{\overset{e}{S}\setminus S} \left(\boldsymbol{v}^{HPq}\right)^T \left\langle \overset{e}{\boldsymbol{r}}(\boldsymbol{u}^{hpq})\right\rangle \mathrm{d}\overset{e}{S} \\ &+ \int\limits_{\overset{e}{S}\setminus S} \psi^{H\Pi\rho}\left\langle \overset{e}{h}(\phi^{h\pi\rho})\right\rangle \mathrm{d}\overset{e}{S},\end{aligned} \tag{19}$$

In this case, the exact solution $(\boldsymbol{u}^{q},\phi^{\rho})$ replaces $(\boldsymbol{u},\phi)$ in equations (15)–(17). Vectors $\boldsymbol{u}^{q}$ and ϕ^{ρ} correspond to the element models MI and EJ of assumed orders $I = q$ and $J = \rho$ (see [13] for details). The infinite values of H,P,Π are replaced with $H = h$, $P = p+1$, and $\Pi = \pi+1$. Additionally, the local coupled solution belongs to: $(\boldsymbol{u}^{HPq},\phi^{H\Pi\rho}) \in U^{HPq}\times\Phi^{H\Pi\rho}$.

In the case of the Dirichlet-type local problems (elements adjacent to the boundary parts W and F of the global domain), the local (element) spaces U^{HPQ} (or U^{HPq}) and $\Phi^{H\Pi\mathrm{P}}$ (or $\Phi^{H\Pi\rho}$) are defined analogously to the global spaces U^{hpq} and $\Phi^{h\pi\rho}$ presented below equation (14), with element volume $\overset{e}{V}$ and element surface parts $\overset{e}{W}$, $\overset{e}{F}$, $\overset{e}{S}$ replacing the global domain quantities V and W, F, S. In the case of the Neumann-type local problems (elements non-adjacent to the boundary parts W and F), these spaces must exclude rigid body motions in the displacement field and underdetermination of the potential field.

With the use of the potential energy definition of equation (1) (completed with equations (2)–(7)), the stationarity equations (18) and (19) can be converted to:

$$\begin{cases}\overset{e}{B}\left(\boldsymbol{v}^{HPQ},\boldsymbol{u}^{HPQ}\right) - \overset{e}{C}\left(\boldsymbol{v}^{HPQ},\phi^{H\Pi\mathrm{P}}\right) = \overset{e}{L}\left(\boldsymbol{v}^{HPQ}\right) \\ \qquad\qquad + \displaystyle\int\limits_{\overset{e}{S}\setminus S} \left(\boldsymbol{v}^{HPQ}\right)^T \left\langle \overset{e}{\boldsymbol{r}}(\boldsymbol{u}^{hpq})\right\rangle \mathrm{d}\overset{e}{S}, \\ \overset{e}{C}\left(\psi^{H\Pi\mathrm{P}},\boldsymbol{u}^{HPQ}\right) + \overset{e}{b}\left(\psi^{H\Pi\mathrm{P}},\phi^{H\Pi\mathrm{P}}\right) = \overset{e}{l}\left(\psi^{H\Pi\mathrm{P}}\right) \\ \qquad\qquad + \displaystyle\int\limits_{\overset{e}{S}\setminus S} \psi^{H\Pi\mathrm{P}}\left\langle \overset{e}{h}(\phi^{h\pi\rho})\right\rangle \mathrm{d}\overset{e}{S}\end{cases} \tag{20}$$

and

$$\begin{cases} \overset{e}{B}\left(\boldsymbol{v}^{HPq},\boldsymbol{u}^{HPq}\right)-\overset{e}{C}\left(\boldsymbol{v}^{HPq},\phi^{H\Pi\rho}\right)=\overset{e}{L}\left(\boldsymbol{v}^{HPq}\right) \\ \qquad +\int\limits_{\overset{e}{S}\setminus S}\left(\boldsymbol{v}^{HPq}\right)^{T}\left\langle\overset{e}{\boldsymbol{r}}(\boldsymbol{u}^{hpq})\right\rangle \mathrm{d}\overset{e}{S}, \\ \overset{e}{C}\left(\psi^{H\Pi\rho},\boldsymbol{u}^{HPq}\right)+\overset{e}{b}\left(\psi^{H\Pi\rho},\phi^{H\Pi\rho}\right)=\overset{e}{l}\left(\psi^{H\Pi\rho}\right) \\ \qquad +\int\limits_{\overset{e}{S}\setminus S}\psi^{H\Pi\rho}\left\langle\overset{e}{h}(\phi^{h\pi\rho})\right\rangle \mathrm{d}\overset{e}{S} \end{cases} \tag{21}$$

The above relations can be used for the determination of the approximated local solutions corresponding to the total error estimation and the approximated local solutions corresponding to the approximation error estimation, respectively.

3.3. Determination of the equilibrated inter-element stresses and charges

The vector of the equilibrated inter-element stresses is defined in the following way:

$$\left\langle\overset{e}{\boldsymbol{r}}(\boldsymbol{u}^{hpq})\right\rangle=\overset{fe}{\boldsymbol{\alpha}}\,\overset{e}{\boldsymbol{r}}\left(\boldsymbol{u}^{hpq}\right)+\overset{ef}{\boldsymbol{\alpha}}\,\overset{f}{\boldsymbol{r}}\left(\boldsymbol{u}^{hpq}\right), \tag{22}$$

where $\overset{e}{\boldsymbol{r}}$ and $\overset{f}{\boldsymbol{r}}$ are the surface stress vector of element e and its neighbour f, while $\overset{fe}{\boldsymbol{\alpha}}$ and $\overset{ef}{\boldsymbol{\alpha}}=\mathbf{1}-\overset{fe}{\boldsymbol{\alpha}}$ are the so-called splitting functions (see [4] for the explanation). By analogy, inter-element equivalent charges can be defined as:

$$\left\langle\overset{e}{h}(\phi^{h\pi\rho})\right\rangle=\overset{fe}{\beta}\,\overset{e}{h}\left(\phi^{h\pi\rho}\right)+\overset{ef}{\beta}\,\overset{f}{h}\left(\phi^{h\pi\rho}\right), \tag{23}$$

where $\overset{e}{h}$ and $\overset{f}{h}$ are equivalent surface charges of the elements e and f. Subsequently, $\overset{fe}{\beta}$ and $\overset{ef}{\beta}=1-\overset{fe}{\beta}$ are the corresponding splitting functions.

To determine the nodal splitting factors $\overset{fe}{\boldsymbol{\alpha}}_k$ and $\overset{fe}{\beta}_k$ of the linear splitting functions $\overset{fe}{\boldsymbol{\alpha}}$ and $\overset{fe}{\beta}$ the following definitions are applied:

$$\overset{fe}{\boldsymbol{\alpha}}=\sum_k\overset{fe}{\boldsymbol{\alpha}}_k\chi_k,\qquad \overset{fe}{\beta}=\sum_k\overset{fe}{\beta}_k\chi_k, \tag{24}$$

where $k=1,2,\ldots,K$ and K is the total number of the vertex nodes in the element, while χ_k are vertex node shape functions.

The starting point for the determination procedure is the load compatibility condition [6] extended for the case of piezoelectricity [11]. The nodal contribution to this condition reads:

$$\begin{aligned}0=&-\overset{e}{B}\left(\boldsymbol{u}^{hpq},\boldsymbol{\chi}_k\right)+\overset{e}{C}\left(\phi^{h\pi\rho},\boldsymbol{\chi}_k\right)+\overset{e}{L}\left(\boldsymbol{\chi}_k\right)\\&+\int\limits_{\overset{e}{S}\setminus S}\boldsymbol{\chi}_k{}^{T}\left\langle\overset{e}{\boldsymbol{r}}\left(\boldsymbol{u}^{hpq}\right)\right\rangle \mathrm{d}\overset{e}{S}.\end{aligned} \tag{25}$$

In the case of an electric field, the external and equivalent charge compatibility condition holds (see [11]). Its nodal contribution is:

$$\begin{aligned}0=&\overset{e}{b}\left(\phi^{h\pi\rho},\chi_k\right)+\overset{e}{C}\left(\boldsymbol{u}^{hpq},\chi_k\right)-\overset{e}{l}\left(\chi_k\right)\\&+\int\limits_{\overset{e}{S}\setminus S}\chi_k\left\langle\overset{e}{h}\left(\phi^{h\pi\rho}\right)\right\rangle \mathrm{d}\overset{e}{S}.\end{aligned} \tag{26}$$

Equations (25) and (26) are valid for the vertex nodes of the hierarchical shell models MI, $I\equiv q\geq 2$ and symmetric-thickness electric models EJ, $J\equiv\rho\geq 1$. We will call such nodes hierarchical vertex nodes and the corresponding vertex shape functions hierarchical vertex shape functions. These two relations are also valid for hierarchical vertex nodes of the transition elements (TR, EJ), where TR $\equiv$ MI/RM.

In the case of the first-order model RM ($q=1$), equation (25) must be modified. Firstly, the hierarchical vertex shape functions must be replaced by the first-order vertex shape functions defined as $\lambda_k=0.5\left(\chi_k+\chi_{k+K/2}\right)$ for $k=1,2,\ldots,K/2$ and $\lambda_k=0.5\left(\chi_{k-K/2}+\chi_k\right)$ for $k=K/2{+}1,K/2{+}2,\ldots,K$ to satisfy equation (10) of no elongation of the lines perpendicular to the shell mid-surface (see [9]). Additionally, equation (25) must be written using the nodal direction consistent with the Reissner-Mindlin no-elongation condition, i.e.,

$$\begin{aligned}0=&-\overset{e}{B}\left(\boldsymbol{u}^{hpq},\boldsymbol{\theta}_k\boldsymbol{\lambda}_k\right)+\overset{e}{C}\left(\phi^{h\pi\rho},\boldsymbol{\theta}_k\boldsymbol{\lambda}_k\right)+\overset{e}{L}\left(\boldsymbol{\theta}_k\boldsymbol{\lambda}_k\right)\\&+\int\limits_{\overset{e}{S}\setminus S}\boldsymbol{\lambda}_k{}^{T}\boldsymbol{\theta}_k^{T}\left\langle\overset{e}{\boldsymbol{r}}\left(\boldsymbol{u}^{hpq}\right)\right\rangle \mathrm{d}\overset{e}{S}\end{aligned} \tag{27}$$

where $\boldsymbol{\theta}_k$ represents the nodal transformation matrix of the global directions ($i=1,2,3$) to the local directions $\alpha=1,2,3$ at the node k. This matrix is consistent with the matrix $\boldsymbol{\theta}=\{\theta_{\alpha i}\}$ introduced for the parametric geometry representation (see Section 2.1).

After substitution of equations (22), (23), and (24), respectively into equations (25) and (26) one can obtain the following directional conditions for the hierarchical vertex nodes corresponding to the mechanical field:

$$\begin{aligned}0=&-\overset{e}{B}\left(\boldsymbol{u}^{hpq},\boldsymbol{\chi}_k\right)+\overset{e}{C}\left(\phi^{h\pi\rho},\boldsymbol{\chi}_k\right)+\overset{e}{L}\left(\boldsymbol{\chi}_k\right)\\&+\sum_f\left[\overset{fe}{\boldsymbol{\alpha}}_k\int\limits_{\overset{ef}{S}}\boldsymbol{\chi}_k{}^{T}\overset{e}{\boldsymbol{r}}\left(\boldsymbol{u}^{hpq}\right)\mathrm{d}\overset{e}{S}+\overset{ef}{\boldsymbol{\alpha}}_k\int\limits_{\overset{ef}{S}}\boldsymbol{\chi}_k{}^{T}\overset{e}{\boldsymbol{r}}\left(\boldsymbol{u}^{hpq}\right)\mathrm{d}\overset{e}{S}\right]\end{aligned} \tag{28}$$

with $\overset{ef}{\boldsymbol{\alpha}}_k=\{\alpha_i\}$, $i=1,2,3$. The scalar condition for the hierarchical vertex nodes of the electric field reads:

$$\begin{aligned}0=&\overset{e}{b}\left(\phi^{h\pi\rho},\chi_k\right)+\overset{e}{C}\left(\boldsymbol{u}^{hpq},\chi_k\right)-\overset{e}{l}\left(\chi_k\right)\\&+\sum_f\left[\overset{fe}{\beta}_k\int\limits_{\overset{ef}{S}}\chi_k\left(\phi^{h\pi\rho}\right)\mathrm{d}\overset{e}{S}+\overset{ef}{\beta}_k\int\limits_{\overset{ef}{S}}\chi_k\left(\phi^{h\pi\rho}\right)\mathrm{d}\overset{e}{S}\right],\end{aligned} \tag{29}$$

where $\overset{ef}{S}$ is a part of $\overset{e}{S}\setminus S$, neighbouring the element f.

In the case of the first-order nodes, the local splitting factors $\overset{fe}{\boldsymbol{\alpha}}_k = \{\alpha_\alpha\}$, $\alpha = 1,2,3$ are in use and equation (28) reads:

$$0 = -\overset{e}{B}\left(\boldsymbol{u}^{hpq}, \boldsymbol{\theta}_k \boldsymbol{\lambda}_k\right) + \overset{e}{C}\left(\phi^{h\pi\rho}, \boldsymbol{\theta}_k \boldsymbol{\lambda}_k\right) + \overset{e}{L}\left(\boldsymbol{\theta}_k \boldsymbol{\lambda}_k\right) + \sum_f \left[\overset{fe}{\alpha}_k \int_{\overset{ef}{S}} \boldsymbol{\lambda}_k{}^T \boldsymbol{\theta}_k^T \overset{e}{\boldsymbol{r}}\left(\boldsymbol{u}^{hpq}\right) \mathrm{d}\overset{e}{S} + \overset{ef}{\alpha}_k \int_{\overset{ef}{S}} \boldsymbol{\lambda}_k{}^T \boldsymbol{\theta}_k^T \overset{e}{\boldsymbol{r}}\left(\boldsymbol{u}^{hpq}\right) \mathrm{d}\overset{e}{S} \right]. \tag{30}$$

The nodal splitting factors $\overset{fe}{\alpha}_k$ and $\overset{ef}{\beta}_k$ can be calculated from the equilibration conditions, i.e., equation (28) (or equation (30)) and equation (29) written for the element patches including elements surrounding the hierarchical or first-order vertex nodes of the domain V (see [6, 7] and [11]).

Note that in this and our previous implementations of ERM, we use averaging when the equilibration conditions become underdetermined. Then, the splitting factors are equal to $1/2$.

4. NUMERICAL EXAMPLES

In our calculations, we will be interested in the effectivity of error estimation using the equilibrated residual method in the case of piezoelectric structures with a complex description of the electro-mechanical field. We will define such effectivity as the ratio of the estimated error value to its exact (or true) value, i.e.,

$$\theta = \frac{\eta}{e}. \tag{31}$$

4.1. Errors and their estimators

The estimated error (or error estimate) of the potential energy will be defined as follows:

$$\begin{aligned} &-\Pi\left(\hat{\boldsymbol{u}}, \hat{\phi}\right) + \Pi\left(\boldsymbol{u}^{hpq}, \phi^{h\pi\rho}\right) \equiv \Pi\left(\hat{\boldsymbol{u}} - \boldsymbol{u}^{hpq}, \hat{\phi} - \phi^{h\pi\rho}\right) \\ &= \frac{1}{2} B\left(\hat{\boldsymbol{u}} - \boldsymbol{u}^{hpq},\ \hat{\phi} - \phi^{h\pi\rho}\right) - \frac{1}{2} C\left(\hat{\boldsymbol{u}} - \boldsymbol{u}^{hpq},\ \hat{\phi} - \phi^{h\pi\rho}\right) \\ &\quad - \frac{1}{2} C\left(\hat{\phi} - \phi^{h\pi\rho},\ \hat{\boldsymbol{u}} - \boldsymbol{u}^{hpq}\right) - \frac{1}{2} b\left(\hat{\phi} - \phi^{hpq},\ \hat{\phi} - \phi^{h\pi\rho}\right) \\ &= \eta_M - \eta_C - \eta_E = \eta. \end{aligned} \tag{32}$$

In the above relation, the difference in potential energies resulting from the estimated solution $\left(\hat{\boldsymbol{u}}, \hat{\phi}\right)$ and the numerical solution $\left(\boldsymbol{u}^{hpq}, \phi^{h\pi\rho}\right)$ was replaced by the equivalent sum of elastic strain energy $1/2B$, electric field energy $1/2b$ and the coupling energy C. We thus introduce three components of the error estimate η (mechanical η_M, electric η_E and electro-mechanical η_C). These components are defined by the total errors at any point within the mechanical field of displacements and electric field of potential:

$$\begin{aligned} \boldsymbol{\eta}^t &= \hat{\boldsymbol{u}} - \boldsymbol{u}^{hpq} = \left(\hat{\boldsymbol{u}} - \boldsymbol{u}^q\right) + \left(\boldsymbol{u}^q - \boldsymbol{u}^{hpq}\right) = \boldsymbol{\eta}^m + \boldsymbol{\eta}^a, \\ \eta^t &= \hat{\phi} - \phi^{h\pi\rho} = \left(\hat{\phi} - \phi^\rho\right) + \left(\phi^\rho - \phi^{h\pi\rho}\right) = \eta^m + \eta^a. \end{aligned} \tag{33}$$

The total errors (index t) can be divided into those due to modelling (index m) and approximation (index a). The estimated solution $\left(\boldsymbol{u}^q, \phi^\rho\right)$ corresponds to the fixed orders q and ρ of the mechanical models MI, RM, TR and the electric model EJ, respectively.

In the case of element components of the above estimators, the exact values of the estimates $\left(\hat{\boldsymbol{u}}, \hat{\phi}\right)$ and $\left(\boldsymbol{u}^q, \phi^\rho\right)$ are replaced by their local (element) FEM approximations, respectively $\left(\boldsymbol{u}^{HPQ}, \phi^{H\Pi P}\right)$ and $\left(\boldsymbol{u}^{HPq}, \phi^{H\Pi\rho}\right)$, in the cases of the total and approximation error estimation. These approximations are obtained from the local problems defined in equations (20) and (21).

Obtaining analogous true error definitions of e, e_M, e_C, e_E requires replacing the ERM-estimated solution $\left(\hat{\boldsymbol{u}}, \hat{\phi}\right)$ with the exact solution $(\boldsymbol{u}, \phi)$ in equation (15). Doing so allows us to determine three components of the error and define total, modelling, and approximation errors, $\boldsymbol{e}^t$, $\boldsymbol{e}^a$, $\boldsymbol{e}^m$, e^t, e^a, e^m, for each of these three components. Note that the exact solution $(\boldsymbol{u}, \phi)$ from equation (13) equals $\left(\boldsymbol{u}^{hpq}, \phi^{h\pi\rho}\right)$ from equation (14) for $1/h, p, q \to \infty$ and $1/h, \pi, \rho \to \infty$. In practice, we use the maximum values possible in our FEM adaptive code instead of the infinite values. This way an overkill mesh is generated and the exact solution $(\boldsymbol{u}, \phi)$ is replaced by $\left(\boldsymbol{u}^{\mathrm{ref}}, \phi^{\mathrm{ref}}\right)$, with maximum possible values of p, π and q, ρ, for the total error calculation. In the case of the approximation error, another overkill mesh is created and $(\boldsymbol{u}, \phi)$ in equation (15) is replaced by $\left(\boldsymbol{u}^{\mathrm{mod}}, \phi^{\mathrm{mod}}\right)$ with maximum possible values of p, π and fixed q, ρ taken from the global problem defined by equation (14).

4.2. Model problem

Our numerical tests concern a square plate of length $l = 3.1414 \cdot 10^{-2}$ m and thickness $t = 0.15 \cdot 10^{-2}$ m.

As the shape, boundary conditions, forces and charges are all symmetric, a quarter of the plate of dimensions $l/2 \times l/2 \times t$ will be analyzed. The applied mesh will consist of $4 \times 4 \times 2$ prismatic elements. We will apply two simple and three complex piezoelectric models. In the simple models, we will apply either hierarchical MI ($I \equiv q = 2$) or first-order RM ($q = 1$) shell models and symmetric-thickness hierarchical electric models EJ ($J \equiv \rho = 2$ for MI) or ($J \equiv \rho = 1$ for RM). In the case of the complex models (Fig. 1), one layer of hierarchical (MI, EJ, $I = 2$, $J = 2$) elements is applied along the plate boundary. Additionally, two layers of (RM, EJ, $J = 1$) elements are employed in the interior of the plate. These two types of elements are connected with one layer of transition elements (TR, EJ, $J = 1$ and 2). In the complex models, we use either the classical, modified or enhanced transition elements.

The piezoelectric properties of the plate correspond to a typical piezoceramic material [22]. Young's modulus is equal to $E = 0.5 \cdot 10^{11}$ N/m^2, and the Poisson's ratio is $\nu = 0.294$.

A normal pressure on the upper surface of the plate is $p = 4 \cdot 10^6$ N/m^2. The lateral sides of the plate are clamped. These sides are also electrically grounded. The plate upper

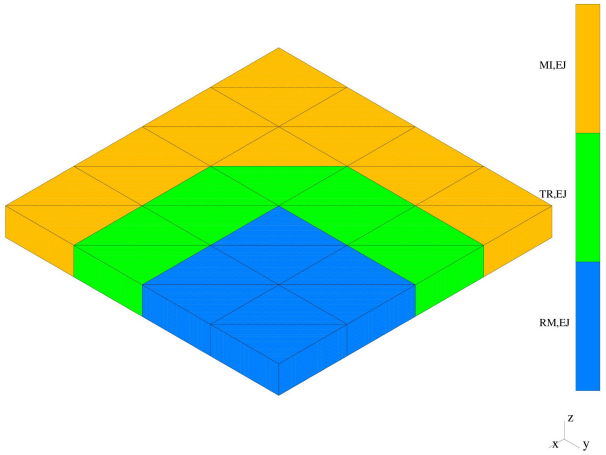

Fig. 1. Complex model of a symmetric quarter of the piezoelectric plate

surface is loaded with electric charges $c = 0.2 \cdot 10^{-1}$ C/m^2. At constant stress, the dielectric permittivity constant equals $\delta = 0.1593 \cdot 10^{-7}$ F/m. At constant stress again, the non-zero piezoelectric constants are $c_{13} = c_{23} = -0.15 \cdot 10^{-9}$ C/N, $c_{33} = 0.3 \cdot 10^{-9}$ C/N and $c_{52} = c_{62} = 0.5 \cdot 10^{-9}$ C/N. In practical engineering calculations, the values of the pressure and electric charges are usually smaller. Here, we applied their maximum possible values as they give mechanical and electric potential energy contributions of the same order (the most numerically demanding case of error estimation – cf. [11]). Note that the values of pressure and charges do not influence our error effectivity calculations due to the linearity of the piezoelectric problem and the relative character of the effectivity indices.

In our effectivity calculations changing values of the longitudinal approximation orders within the mechanical and electric fields will be applied: $p = \pi = 1, 2, 3, \ldots$, $p_{\max} = \pi_{\max} = 7$ or 8.

In the case of overkill meshes mentioned in Section 4.1, the calculation of $(\boldsymbol{u}^{\mathrm{ref}}, \phi^{\mathrm{ref}})$ is performed for p, $\pi = 9$ and q, $\rho = 6$, while obtainment of $(\boldsymbol{u}^{\mathrm{mod}}, \phi^{\mathrm{mod}})$ requires p, $\pi = 9$ with fixed q and ρ taken as for $(\boldsymbol{u}^{hpq}, \phi^{h\pi\rho})$ from equation (14). For both overkill meshes, the longitudinal division numbers are equal to $m = l/2h = 9$.

Note that our model problem does not include singularities. To check effectivity indices in such cases, other model problems, e.g., L-shaped domain piezoelectric plate, can be proposed for future research.

4.3. Results and discussion

To obtain the results in the tables presented below, values of the mechanical, coupling, and electric parts of the global ERM estimators are applied including their total, approximating, and modelling components. These values result from a collection of the local ERM solutions of the problems defined in equations (20) and (21) for the total and approximation error estimators. The modelling error estimator is obtained as a difference between the previous two. In the local problems, all 18 vertex displacement degrees of freedom are constrained. Also, one electric potential degree of freedom is constrained. In the local problems, longitudinal orders of approximation P and Π are increased by 1 concerning the global values p and π, in the case of total and approximation error estimation. Vertical orders Q and P are increased by 1 concerning the global values of q and ρ, in the case of the total error estimation.

Table 1 presents global effectivity results for the complex model (MI/TR/RM, EJ) employing the classical transition elements. The presented results can be confronted with [14] where different mesh density is applied.

In Table 2 the global effectivity results for three parts of the estimator and three components of each part are displayed. They correspond to the complex model (MI/TR/RM, EJ) with the modified transition elements employed.

Table 3 presents global effectivity results for all parts and all components of the estimator. The results concern the complex model (MI/TR/RM, EJ) employing the enhanced transition elements.

Table 1

Global effectivities in the case of a complex piezoelectric model with classical transition elements (MI/TR/RM, EJ) (in the global problem $q = \rho = 1$ and $q = \rho = 2$, $p = \pi = var$, $m = 4$; in the local problems in the mechanical field: 18 vertex constraints, $H = h$, $P = p + 1$, $Q = q + 1$ or $Q = q$, in the electric field: 1 vertex constraint, $H = h$, $\Pi = \pi + 1$, P $= \rho + 1$ or P $= \rho$)

Part of estimator	Component of a part	Values of the degrees of approximation p or π						
		1	2	3	4	5	6	7
Mechanical	Total	0.77	2.15	1.03	0.97	1.01	1.00	1.01
	Approximation	0.73	2.30	1.13	0.94	0.96	1.04	1.32
	Modelling	0.78	1.56	1.02	1.00	1.01	1.01	1.01
Coupling	Total	1.01	2.99	1.14	1.10	1.09	1.08	1.08
	Approximation	1.29	1.73	0.79	0.77	0.83	0.90	1.16
	Modelling	0.29	1.09	1.07	1.07	1.08	1.08	1.08
Electric	Total	1.12	1.25	0.93	0.93	0.93	0.92	0.92
	Approximation	1.20	1.56	0.85	0.84	0.88	0.94	1.16
	Modelling	1.33	0.98	0.95	0.93	0.93	0.92	0.92

Table 2

Global effectivities in the case of a complex piezoelectric model with modified transition elements (M*I*/TR/RM, E*J*) (in the global problem $q = \rho = 1$ and $q = \rho = 2$, $p = \pi = var$, $m = 4$; in the local problems in the mechanical field: 18 vertex constraints, $H = h$, $P = p + 1$, $Q = q + 1$ or $Q = q$, in the electric field: 1 vertex constraint, $H = h$, $\Pi = \pi + 1$, $\mathrm{P} = \rho + 1$ or $\mathrm{P} = \rho$)

Part of estimator	Component of a part	Values of the degrees of approximation p or π						
		1	2	3	4	5	6	7
Mechanical	Total	0.82	2.16	1.06	1.05	1.08	1.08	1.10
	Approximation	0.78	2.34	1.26	1.32	1.88	1.87	1.60
	Modelling	0.94	1.54	1.03	1.03	1.04	1.04	1.05
Coupling	Total	1.31	2.74	1.11	1.10	1.07	1.07	1.07
	Approximation	1.67	2.52	0.83	0.82	0.96	1.19	2.04
	Modelling	0.46	1.18	1.06	1.07	1.07	1.08	1.08
Electric	Total	1.32	2.22	0.94	0.93	0.93	0.93	0.93
	Approximation	1.41	3.11	0.91	0.86	0.95	1.09	1.70
	Modelling	1.61	1.20	0.94	0.93	0.93	0.92	0.92

Table 3

Global effectivities in the case of a complex piezoelectric model with enhanced transition elements (M*I*/TR/RM, E*J*) (in the global problem $q = \rho = 1$ and $q = \rho = 2$, $p = \pi = var$, $m = 4$; in the local problems in the mechanical field: 18 vertex constraints, $H = h$,$P = p + 1$, $Q = q + 1$ or $Q = q$, in the electric field: 1 vertex constraint, $H = h$, $\Pi = \pi + 1$, $\mathrm{P} = \rho + 1$ or $\mathrm{P} = \rho$)

Part of estimator	Component of a part	Values of the degrees of approximation p or π						
		1	2	3	4	5	6	7
Mechanical	Total	0.82	2.17	1.06	1.05	1.07	1.07	1.09
	Approximation	0.78	2.35	1.28	1.38	1.95	1.94	1.67
	Modelling	0.95	1.56	1.04	1.04	1.05	1.05	1.06
Coupling	Total	1.31	2.84	1.11	1.09	1.07	1.07	1.07
	Approximation	1.67	2.52	0.83	0.82	0.95	1.18	2.02
	Modelling	0.46	1.18	1.07	1.07	1.07	1.08	1.08
Electric	Total	1.32	2.12	0.94	0.93	0.93	0.93	0.93
	Approximation	1.40	3.10	0.91	0.86	0.95	1.09	1.71
	Modelling	1.61	1.20	0.94	0.93	0.93	0.92	0.92

For all three piezoelectric complex models, for the longitudinal approximation orders $p \geq 3$ and $\pi \geq 3$, almost all total and modelling components of the estimator are between 0.9 and 1.1. For the same range, most of the approximation components of the estimator are in the range between 0.8 and 2.0. This means that the true and estimated error values are either close (the range 0.9–1.1) or similar (the range 0.8–2.0) to the desired effectivity value equal to 1.0. The best results for the approximation components are obtained with the use of the classical transition elements.

The first general remark we would like to make is that acceptable ERM global effectivities are between 1.0 and 3.0 (compare [23]). Note also that higher values of the global effectivities can be observed for thin structures or small errors, for example. In our model problem, the approximation error is ten times less than the modelling error. As a result, our effectivities for the approximation components are worse than for the modelling components. Another general remark concerns some deterioration of the effectivity values with the increase of the approximation order. The deterioration usually results from insufficient quality of the true error value obtained from the overkill mesh. This is also our case – we were not able to obtain better true error results due to our code capabilities.

In Tables 4 and 5, to further assess by comparison the quality of the estimation for the above three complex models, we present the effectivity results for simple (basic) models (M*I*, E*J*) and (RM, E*J*).

Note that the results presented in Table 4 for the coupling and electric parts of the estimator can be improved (effectivities can move closer to 1.0) using the tuning procedure presented in [11].

It results from a comparison of Tables 1–3 and Tables 4–5 that all three complex models of the piezoelectric plate deliver effectivities of the same quality as two basic (homogenous) piezoelectric models. For all estimator components, except those requiring the application of a tuning procedure, the results are either close (less than 10% difference) or similar (up to 50%

Table 4

Global effectivities in the case of a simple piezoelectric plate model (MI, EJ) (in the global problem $q = \rho = 2$, $p = \pi = var$, $m = 4$; in the local problems in the mechanical field: 18 vertex constraints, $H = h$, $P = p + 1$, $Q = q + 1$ or $Q = q$, in the electric field: 1 vertex constraint, $H = h$, $\Pi = \pi + 1$, $\mathrm{P} = \rho + 1$ or $\mathrm{P} = \rho$)

Part of estimator	Component of a part	Values of the degrees of approximation p or π						
		1	2	3	4	5	6	7
Mechanical	Total	0.76	2.27	1.07	1.01	1.02	1.02	1.03
	Approximation	0.76	2.35	1.15	0.92	0.92	1.00	1.22
	Modelling	0.93	1.79	1.03	1.02	1.03	1.02	1.03
Coupling	Total	1.01	1.83	0.79	0.73	0.71	0.62	0.50
	Approximation	1.01	1.86	0.79	0.76	0.81	0.88	1.07
	Modelling	0.43	1.03	0.40	0.32	0.39	0.31	0.34
Electric	Total	1.13	1.54	0.83	0.77	0.69	0.58	0.47
	Approximation	1.14	1.61	0.85	0.84	0.87	0.94	1.10
	Modelling	0.71	0.71	0.47	0.42	0.41	0.39	0.40

Table 5

Global effectivities in the case of a simple piezoelectric plate model (RM, EJ) (in the global problem $q = \rho = 1$, $p = \pi = var$, $m = 4$; in the local problems in the mechanical field: 18 vertex constraints, $H = h$, $P = p + 1$, $Q = q + 1$ or $Q = q$, in the electric field: 1 vertex constraint, $H = h$, $\Pi = \pi + 1$, $\mathrm{P} = \rho + 1$ or $\mathrm{P} = \rho$)

Part of estimator	Component of a part	Values of the degrees of approximation p or π						
		1	2	3	4	5	6	7
Mechanical	Total	0.80	1.80	0.95	0,93	0,93	0.92	0.92
	Approximation	0.68	2.13	1.87	1.35	1.65	1.24	1.87
	Modelling	0.85	1.41	0.95	0.93	0.93	0.92	0.92
Coupling	Total	1.00	1.37	0.99	1.00	1.01	1.01	1.01
	Approximation	2.14	5.00	0.86	1.36	1.23	1.99	1.48
	Modelling	0.67	1.22	1.00	1.00	1.01	1.01	1.01
Electric	Total	1.09	1.12	0.98	0.98	0.98	0.98	0.98
	Approximation	1.36	3.04	1.26	1.52	1.38	1.95	1.16
	Modelling	0.73	1.07	0.98	0.98	0.98	0.98	0.98

difference) for the total and modelling components, and the approximation components, respectively.

It can be noticed that the effectivities are higher for the complex models than for the simple (homogenous) models. This is consistent with the observation of other researchers concerning numerical models with different orders of approximation in neighbouring elements.

To further assess the quality of the estimation for coupled problems one can compare the results presented in Tables 1–3 with the analogous results for uncoupled problems for which the upper bound of the estimation holds. In Table 6 we consider three complex mechanical models with different (classical, modified, enhanced) transition elements employed. Also, the common results for the complex dielectric model are presented. In this model, $J = \rho = 2$ is applied to two boundary layers of elements and $J = \rho = 1$ to internal layers.

Comparing the results from Table 6 for three uncoupled mechanical problems one can notice their closeness (about 10% difference) or similarity (less than 50% difference) in the case of total and modelling components and the case of approximation components, respectively. The analogous closeness and similarity can be seen by comparing these results with the analogous results for three coupled piezoelectric problems presented in Tables 1–3. Additionally, such closeness (total and modelling components) or similarity (approximation components) can be observed for the common uncoupled problem of dielectricity from the above table and the results presented in Tables 1–3 for three coupled piezoelectric problems.

Table 6

Global effectivities – three complex models for uncoupled problems (M*I*/TR/RM) and (E*J*) (in the global elasticity problem $q = 1$ and $q = 2$, $p = var$, $m = 4$; in the local problems: 18 vertex constraints, $H = h$, $P = p + 1$, $Q = q + 1$ or $Q = q$, and in the dielectric global problem: $\rho = 1$ and $\rho = 2$, $\pi = var$, $m = 4$, in the local problems: 1 vertex constraint, $H = h$, $\Pi = \pi + 1$, $\mathrm{P} = \rho + 1$ or $\mathrm{P} = \rho$)

Uncoupled problem type	Part of estimator	Component of a part	Values of the degrees of approximation p or π							
			1	2	3	4	5	6	7	8
Elasticity (classical transition model)	Mechanical	Total	0.65	1.81	1.03	0.97	0.98	0.96	0.95	0.94
		Approximation	0.64	1.81	1.05	0.99	1.04	1.13	1.23	1.51
		Modelling	0.91	1.78	1.02	0.96	0.96	0.94	0.95	0.93
Elasticity (modified transition model)	Mechanical	Total	0.65	1.84	1.05	1.00	1.01	1.00	1.00	0.99
		Approximation	0.64	1.89	1.20	1.38	1.32	1.25	1.44	1.47
		Modelling	0.86	1.57	0.94	0.90	0.91	0.98	0.98	0.89
Elasticity (enhanced transition model)	Mechanical	Total	0.65	1.84	1.05	0.99	1.00	0.99	0.99	0.98
		Approximation	0.65	1.86	1.08	1.05	1.15	1.35	1.41	1.81
		Modelling	0.91	1.72	1.02	0.98	0.98	0.97	0.97	0.96
Dielectricity	Electric	Total	1.59	1.82	1.01	1.01	1.00	1.01	1.01	1.01
		Approximation	1.58	2.52	1.09	1.13	1.04	1.04	1.02	1.21
		Modelling	2.16	1.11	1.00	1.00	1.00	1.01	1.01	1.01

5. CONCLUSIONS

The theoretical considerations and calculations in model examples indicate that the equilibrated residual method (ERM) can be applied to complex models of piezoelectrics in which the mechanical field is described by the hierarchical, first-order, and transition shell models, and the electric field by the hierarchical symmetric-thickness model.

The presented effectivities of error estimation using the equilibrated residual method in stationary problems of complex piezoelectric models are either close (less than 10% difference) or similar (up to 50% difference) to the cases of homogeneous models of piezoelectrics and the cases of uncoupled problems of elasticity (elastostatics) and dielectricity (electrostatics).

REFERENCES

[1] D.W. Kelly, "The self-equilibration of residuals and complementary a posteriori error estimates in the finite element method," *Int. J. Numer. Methods Eng.*, vol. 20, no. 8, pp. 1491–1506, 1984.

[2] R.E. Bank and A. Weiser, "Some a posteriori error estimations for elliptic partial differential equations," *Math.Comput.*, vol. 44, pp. 283–301, 1985.

[3] P. Ladeveze and L. Leguillon, "Error estimate procedure in the finite element method and applications," *SIAM J. Numer. Anal.*, vol. 20, pp. 485–509, 1983.

[4] M. Ainsworth and J.T. Oden, "A procedure for a posteriori error estimation for $h - p$ finite element methods," *Comput. Meth. Appl. Mech. Eng.*, vol. 101, pp. 73–96, 1992.

[5] M. Ainsworth and J.T. Oden, "A posteriori error estimators for second order elliptic systems: Part 1. Theoretical foundations and a posteriori error analysis," *Comput. Math. Appl.*, vol. 25, no. 2, pp. 101–113, 1993.

[6] M. Ainsworth and J.T. Oden, "A posteriori error estimators for second order elliptic systems: Part 2. An optimal order process for calculating self-equilibrating fluxes," *Comput. Math. Appl.*, vol. 26, no. 9, pp. 75–87, 1993.

[7] M. Ainsworth, J.T. Oden, and W. Wu, "A posteriori error estimation for $h - p$ approximations in elastostatics," *Appl. Numer. Math.*, vol. 14, pp. 23–55, 1994.

[8] J.T. Oden and J.R. Cho, "Adaptive *hpq*-finite element methods of hierarchical models for plate- and shell-like structures," *Comput. Meth. Appl. Mech. Eng.*, vol. 136, pp. 317–345, 1996.

[9] G. Zboiński, "Adaptive *hpq* finite element methods for the analysis of 3D-based models of complex structures. Part 2. A posteriori error estimation," *Comput. Meth. Appl. Mech. Eng.*, vol. 267, pp. 531–565, 2013.

[10] G. Zboiński, "Adaptive modeling and simulation of elastic, dielectric and piezoelectric problems" in *Finite Element Method. Simulation, Numerical Analysis and Solution Techniques*, R. Pacurar (Ed.), InTech, Rijeka (Croatia), 2018, pp. 157–192.

[11] G. Zboiński, "Tuning of the equilibrated residual method for applications in general, direct and inverse piezoelectricity," *J. Theor. Appl. Mech.*, vol. 62, no. 2, pp. 219–230, 2024.

[12] G. Zboiński, "Tuning of the equilibrated residual method for applications in elasticity, dielectricity and piezoelectricity" in *AIP Conf. Proc.*, 2020, vol. 2239, p. 020050.

[13] G. Zboiński. "Problems of hierarchical modeling and *hp*-adaptive finite element analysis in elasticity, dielectricity and piezoelectricity" in *Perusal of the Finite Element Method*. R. Petrova (Ed.), InTech, Rijeka (Croatia), 2016, pp. 1–29.

[14] M. Zielińska and G. Zboiński, "Szacowanie błędów w adaptacyjnej analizie złożonych modeli piezoelektryków," in *Aspekty komputerowego wspomagania projektowania, wytwarzania i eksploatacji. Część 4*, R. Trębiński and D. Rodzik (Eds), Wojskowa Akademia Techniczna, Warszawa, 2024, pp. 151–162.

[15] B.A. Szabó and G.J. Sahrmann, "Hierarchic plate and shell models based on p-extension," *Int. J. Numer. Methods Eng.*, vol. 26, pp. 1855–1881, 1988.

[16] L. Demkowicz, *Computing with hp-Adaptive Finite Elements. Vol. 1. One- and Two-Dimensional Elliptic and Maxwell Problems*, Chapman & Hall/CRC: Boca Raton, FL, 2007.

[17] G. Zboiński and M. Zielińska, "3d-Based Transition *hpq*/*hp*-Adaptive Finite Elements for Analysis of Piezoelectrics," *Appl. Sci.*, vol. 11, p. 4062, 2021.

[18] G. Zboiński and W. Ostachowicz, "An Algorithm of a Family of 3D-Based, Solid-to-Shell, *hpq*/*hp*-Adaptive Finite Elements," *J. Theor. Appl. Mech.*, vol. 38, pp. 791–806, 2000.

[19] M. Zielińska, "Analiza struktur sprężystych adaptacyjną metodą elementów skończonych z wykorzystaniem bryłowo-powłokowych elementów przejściowych," Ph.D. dissertation, Uniwersytet Warmińsko-Mazurski w Olsztynie, Olsztyn, 2016 (in Polish).

[20] G. Zboiński, "Adaptive *hpq* finite element methods for the analysis of 3D-based models of complex structures. Part 1 Hierarchical modelling and approximation," *Comput. Meth. Appl. Mech. Eng.*, vol. 199, pp. 2913–2940, 2010.

[21] G. Zboiński, "3D-based hierarchical models and *hpq*-approximations for adaptive finite element method of Laplace problems as exemplified by linear dielectricity," *Comput. Meth. Appl. Mech. Eng.*, vol. 78, pp. 2468–2511, 2019.

[22] A. Premount, *Mechatronics. Dynamics of Electromechanical and Piezoelectric Systems*, Springer: Dordrecht, 2006.

[23] M. Ainsworth and J.T. Oden. *A Posteriori Error Estimation in Finite Element Analysis*, Wiley: New York, 2000.